Green-Energy-Powered Cognitive Radio Networks: Joint Time and Power Allocation

CHI XU, Shenyang Institute of Automation, Chinese Academy of Sciences, and University of Chinese Academy of Sciences
WEI LIANG and HAIBIN YU, Shenyang Institute of Automation, Chinese Academy of Sciences

This article studies a green-energy-powered cognitive radio network (GCRN) in an underlay paradigm, wherein multiple battery-free secondary users (SUs) capture both the spectrum and the energy of primary users (PUs) to communicate with an access point (AP). By time division multiple access, each SU transmits data to AP in the allocated time and harvests energy from the RF signals of PUs otherwise, all in the same licensed spectrum concurrently with PUs. Thus, the transmit power of each SU is jointly constrained by the peak interference power at PU and the harvested energy of SU. With the formulated green coexistence paradigm, we investigate the sum-throughput maximization problem with respect to time and power allocation, which is non-convex. To obtain the optimal resource allocation, we propose a joint optimal time and power allocation (JOTPA) algorithm that first transforms the original problem into a convex optimization problem with respect to time and energy allocation, and then solve it by iterative Lagrange dual decomposition. To comprehensively evaluate the performance of the GCRN with JOTPA, we deploy the GCRN in three typical scenarios and compare JOTPA with the equal time and optimal power allocation (ETOPA) algorithm. Extensive simulations show that the deployment of the GCRN significantly influences the throughput performance and JOTPA outperforms ETOPA under all considered scenarios.

CCS Concepts: • **Networks** → **Network components**; **Network algorithms**; *Cognitive radios*; *Network resources allocation*;

Additional Key Words and Phrases: Cognitive radio networks, resource allocation, green energy, energy harvesting, throughput

ACM Reference format:
Chi Xu, Wei Liang, and Haibin Yu. 2017. Green-Energy-Powered Cognitive Radio Networks: Joint Time and Power Allocation. *ACM Trans. Embed. Comput. Syst.* 17, 1, Article 13 (August 2017), 18 pages.
https://doi.org/10.1145/3092949

1 INTRODUCTION

Traditional energy-constrained wireless networks, such as wireless sensor networks (WSNs), are typically powered by finite capacity batteries, which bring about the problem of limited network

This work was supported by the National Natural Science Foundation of China under Grant 61233007, Grant 61533015, and Grant 71661147005.
Authors' addresses: C. Xu, the State Key Laboratory of Robotics and the Key Laboratory of Networked Control Systems, Shenyang Institute of Automation, Chinese Academy of Sciences, Shenyang 110016, China, and University of Chinese Academy of Sciences, Beijing 100049, China; email: xuchi@sia.cn; W. Liang and H. Yu (Corresponding author), the State Key Laboratory of Robotics and the Key Laboratory of Networked Control Systems, Shenyang Institute of Automation, Chinese Academy of Sciences, Shenyang 110016, China; emails: {weiliang, yhb}@sia.cn.

https://doi.org/10.1145/3092949

lifetime or frequent battery recharging (Gu et al. 2014). To facilitate energy-constrained problems and decrease carbon emissions, energy harvesting is proposed as a promising technique, since it can provide perpetual energy supply in theory. Conventional energy harvesting mainly capture energy from the natural renewable energy sources such as solar, wind, and vibration, which are mostly random and unstable. With the extensive deployments of wireless networks, the RF signals radiated by ambient transmitters are dramatically increasing and therefore can be captured for energy supply. Thus, RF energy harvesting is more flexible, predictable, and sustainable than conventional energy harvesting. Benefiting from these advantages, wireless power transfer (WPT), wireless powered communication networks (WPCNs), and simultaneous wireless information and power transfer (SWIPT) are extensively studied (Bi et al. 2015).

When the secondary users (SUs) in cognitive radio networks (CRNs) own the capacity of energy harvesting, the RF signals of primary users (PUs) are no longer interference for SUs but can be regarded as a green energy source for energy harvesting. In this way, SUs will not only utilize the spectrum licensed to PUs, but also the RF energy radiated by PUs. Motivated by this, we study the optimal resource allocation of green-energy-powered CRNs (GCRNs) to enhance both spectrum efficiency and green energy utilization in this article.

To be specific, we consider a GCRN with an access point (AP) and multiple battery-free SUs coexisting with a pair of PUs in an underlay paradigm. SUs without constant energy sources are all powered by harvesting energies from the RF signals of the PU transmitter (PT). With the harvested energies, SUs employ time division multiple access (TDMA) to transmit data to AP in the licensed spectrum concurrently with PUs. Besides the allocated transmission duration, SUs continuously harvest energies from PT in the licensed spectrum. In this way, the transmit powers of SUs are subject to not only the interference power constraint of the PU receiver (PR) as in common underlay CRNs, but also the harvested energy constraints of SUs imposed by energy harvesting. Under this setup, we investigate a sum-throughput maximization problem in terms of time and power allocation. However, this problem is non-convex, which makes it difficult to address. By introducing an auxiliary optimization variable, we equivalently convert the original non-convex problem into a convex optimization problem in terms of time and energy allocation. Then, we employ the Lagrange dual decomposition method to iteratively solve the transformed problem. The proposed algorithm is summarized as joint optimal time and power allocation (JOTPA) algorithm. Finally, we design three typical deployments to comprehensively evaluate the performance of the GCRN, and compare JOTPA with an equal time optimal power allocation (ETOPA) algorithm in extensive simulations.

The main contributions and results of this article can be summarized as follows:

- We propose a green underlay coexistence paradigm, in which multiple battery-free SUs harvest both spectrum and energy from PUs to enhance spectrum efficiency and green energy utilization.
- With the proposed GCRN, we formulate the sum-throughput maximization problem in terms of time and power allocation. To solve this problem, we first prove that the sum-throughput is maximized only when a frame is completely allocated, and then propose the JOTPA algorithm to obtain the optimal solution.
- The impacts of different deployments on the throughput of each SU and the sum-throughput of the GCRN are investigated. It is observed that SUs close to PT and AP but far from PR can contribute more throughput to the sum-throughput than other SUs. This observation can guide us to deploy the GCRN properly.
- The GCRN cannot always benefit from PT, since too large transmit power of PT will seriously interfere with AP even though the harvested energies of SUs are enhanced.

Moreover, the GCRN obtains limited sum-throughput if the interference power constraint of PR is strict; otherwise the GCRN is equivalent to a WPCN if the constraint is slack. Thus, the GCRN should be configured according to the setup of PUs.

—JOTPA outperforms ETOPA under all considered scenarios. Specifically, JOTPA can satisfy large number of SUs without sum-throughput decreasing, while ETOPA cannot, as the sum-throughput may decrease with SUs increasing. Moreover, the green energy utilization of JOTPA is also higher than that of ETOPA.

The rest of this article is organized as follows. Section 2 reviews the resource allocation in different types of wireless networks. Section 3 presents the system model of the GCRN. Section 4 formulates the sum-throughput maximization problem and proposes the JOTPA algorithm to solve it. Simulation results are presented and discussed in Section 5, followed by the conclusions in Section 6.

2 RELATED WORK

Resource allocation regarding spectrum/channels, rate, power, and time has been well studied for various kinds of energy harvesting wireless networks, such as cellular networks (Jangsher et al. 2015; Lohani et al. 2016), WPCNs (Ju and Zhang 2014a, 2014b; Kang et al. 2015; Hadzi-Velkov et al. 2016; Cheng et al. 2016), WSNs (Liu et al. 2010; Wang et al. 2015), and CRNs (Huang et al. 2015).

Specifically, Jangsher et al. (2015) study joint resource blocks and power allocation of cellular networks with energy harvesting relay powered by non-intended solar energy, while Lohani et al. (2016) study joint power and time allocation of cellular networks, wherein users are powered by base station or relays with intended WPT. Ju and Zhang (2014b) and Kang et al. (2015) study time allocation for sum-throughput maximization of half-duplex and full-duplex WPCNs, respectively. Furthermore, Hadzi-Velkov et al. (2016) and Ju and Zhang (2014a) study joint power and time allocation for sum-throughput maximization of half-duplex and full-duplex WPCNs, respectively. Recently, with the aim of proportional fairness, Cheng et al. (2016) study joint power and time allocation for utility maximization of full-duplex WPCNs. Additionally, Liu et al. (2010) study routing and rate control for joint energy management and resource allocation of rechargeable WSNs.

However, the aforementioned works do not take into account the spectrum scarcity problem. In contrast, CRNs, no matter in interweave, underlay, or overlay paradigm (Goldsmith et al. 2009), do not suffer from such a problem seriously. The resource allocation of CRNs is an essential but challenging issue. Liang et al. (2008) study the time allocation of interweave CRNs by investigating the sensing-throughput tradeoff, while Kang et al. (2011) study the power allocation of underlay CRNs by convex optimization technique. Moreover, Huang et al. (2006), Wu and Tsang. (2009), and Wang et al. (2012) study the resource allocation of CRNs by game theory.

When energy harvesting is adopted in CRNs, resource allocation becomes more challenging as both energy and spectrum resources are limited. The energy sources can be renewable energy (Chung et al. 2014; Usman and Koo 2014; Yin et al. 2015; He and Zhao 2015; Zhang and Chen 2016), the intended RF signals by WPT (Lee and Zhang 2015; Xu et al. 2016; Yin et al. 2017), and the non-intended RF signals of PUs (Lee et al. 2013; Wang et al. 2015; Rakovic et al. 2015; Zheng et al. 2016; Xu et al. 2017). With different energy sources, the resource allocation of CRNs with energy harvesting are studied as follows.

—Renewable energy sources such as solar and wind are the most widely used energy sources for energy harvesting. This kind of energy sources is green for SUs but may be random and

unstable as energy arrivals in nature are usually uncertain. Chung et al. (2014) optimize the sensing time to maximize the throughput of interweave CRNs. Furthermore, Yin et al. (2015) optimize both harvesting time and sensing time by studying the harvesting-sensing-throughput tradeoff. To maximize the throughput of underlay CRNs, He and Zhao (2015) perform optimal power allocation by recursive water-filling. With the aim of minimizing the average buffer delay, Zhang and Chen (2016) study the power allocation of underlay CRNs. Moreover, Usman and Koo (2014) maximizes the outage throughput of a hybrid interweave and underlay CRN by Markov decision process.

— To provide sustainable and sufficient energy supply, intended WPT can be applied in CRNs to wirelessly charge SUs. However, WPT is not green as it needs constant energy supply. Moreover, the power of WPT in the licensed spectrum must be strictly controlled to protect PUs if there is no dedicated spectrum for WPT. Lee and Zhang (2015) investigate joint power and time allocation for sum-throughput maximization of CRNs, wherein a hybrid AP performs information transmission for PUs as well as WPT to SUs in an overlay paradigm or only WPT to SUs in an underlay paradigm. Similarly, Yin et al. (2017) study joint power and time allocation for energy efficiency maximization of overlay CRNs. Moreover, Xu et al. (2016) study joint power and time allocation for outage minimization of multihop underlay CRNs, wherein a power beacon performs WPT to all SUs.

— As PUs share the licensed spectrum with SUs, the RF energy of PUs can also be captured by SUs for energy harvesting. Although the RF signals of PUs are not intended for SUs, they are green and usually predictable for SUs. Lee et al. (2013) study the throughput maximization of interweave CRNs, wherein SUs opportunistically harvest energy from the ambient active PUs. Wang et al. (2015) optimize time and power allocation to maximize the ergodic throughput of dual-hop overlay CRNs, wherein SUs harvest energy from PUs, serve as relays for PUs, and communicate with other SUs. Rakovic et al. (2015) and Zheng et al. (2016) investigate the optimal time allocation for throughput maximization of single-hop underlay CRNs under the outage constraint and the interference power constraint of PUs, respectively. More recently, Xu et al. (2017) study joint time and power allocation for end-to-end throughput of multi-hop underlay CRNs.

By comparing all the above works, we can observe that, although considerable efforts have been conducted on the resource allocation of different wireless networks, the multiuser resource allocation of underlay GCRNs still remains an open research topic. Thus, this article studies joint time and power allocation for sum-throughput maximization of underlay GCRNs. In the following, we summarize four major differences between this article and previous works. First, different from previous works that ignore either spectrum scarcity or green energy utilization problem, this article takes both issues into consideration to enhance both spectrum efficiency and energy efficiency. Second, conventional energy harvesting mainly depends on the unstable renewable energy sources, while this article employs RF energy harvesting from PUs to benefit SUs with predictable and sustainable energy supply. Meanwhile, unlike common CRNs that regard PUs as interference, the GCRN treats PUs as friends that provide both spectrum and energy. Thus, we indeed study a novel green coexistence paradigm for PUs and SUs. Third, WPCNs are powered by intended but non-green WPT while the proposed GCRN completely lives on the non-intended but green energy of PUs. Thus, unlike the proactive resource allocation of WPCNs that provide sufficient and on-demand energy, the resource allocation of the GCRN is reactive for the given setup of PUs. Finally, the studied GCRN does not suffer from the "doubly near-far" problem as in WPCNs (Ju and Zhang 2014b). Thus, to deploy the GCRN properly, we further study how the setup of PUs and the deployment of SUs influence the GCRN.

Table 1. Summary of Key Notations

Notation	Defination
M	Number of SUs
N	Number of frames
T	Length of a frame
P_t	Transmit power of PT
I_p	Peak interference power at PR
τ_k	Transmission time allocated to SU_k
P_k	Transmit power allocated to SU_k
e_k	Transmit energy allocated to SU_k
E_k	Harvested energy of SU_k
g_k	Channel power gain on the information link from SU_k to AP
h_k	Channel power gain on the energy link from PT to SU_k and AP
f_k	Channel power gain on the interference link from SU_k to PR
N_0	Noise power
ξ	Energy conversion efficiency
$\boldsymbol{\tau}$	Time allocation vector
$\boldsymbol{\mathcal{P}}$	Power allocation vector
$\boldsymbol{e}$	Energy allocation vector
$\mathcal{R}$	Sum-throughput
α	Path loss exponent
d_0	Reference distance

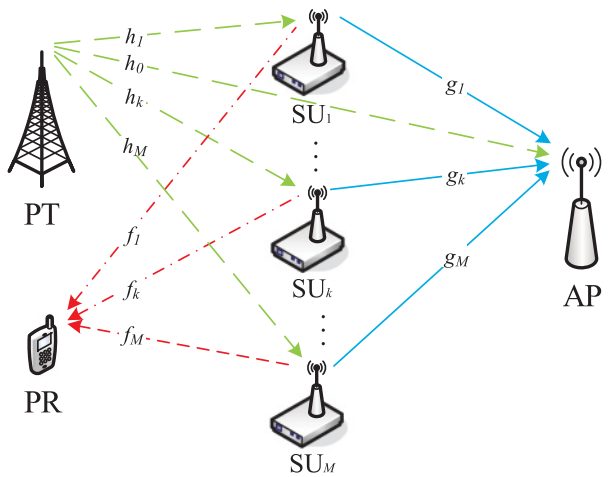

Fig. 1. System model.

3 SYSTEM MODEL

In this section, we formulate the green coexistence paradigm for PUs and SUs. For the ease of presentation, the key mathematical notations are summarized in Table 1.

As shown in Figure 1, we consider an underlay GCRN that consists of an AP and M battery-free SUs sharing the same licensed spectrum with a pair of PUs (i.e., PT and PR). The transmit power of PT is P_t and the peak interference power that PR can tolerate is I_p. AP is powered by an on-grid energy source, while SUs do not own constant energy sources. All SUs harvest energies from the

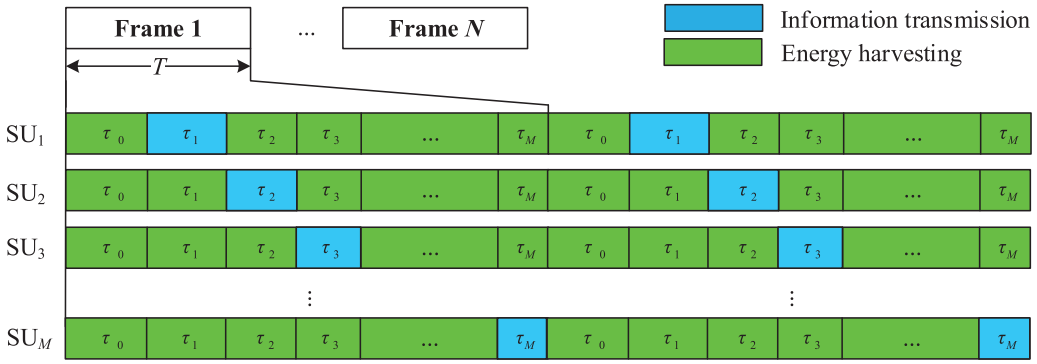

Fig. 2. Frame structure.

RF signals of PT in the licensed spectrum, which means they are completely powered by the green energy. The harvested energy of each SU is kept in a supercapacitor that has the advantages of small form factor and fast charging, since it can be trickle-charged by RF signals without complex charging circuitry and has high charge-discharge efficiency without suffering from memory effect (Sudevalayam and Kulkarni 2011).

Each SU with a single antenna works in the half-duplex mode (i.e., SU can only harvest, receive or transmit at one time) and employs the time-switching scheme to switch between energy harvesting and information transmission. The transmission durations of SUs are allocated by AP as shown in Figure 2, where the allocated time for SU_k ($\forall k \in \{1, \ldots, M\}$) is denoted as τ_k ($0 \leq \tau_k \leq T$). In this way, the total allocated time in a frame satisfies

$$\sum_{k=0}^{M} \tau_k \leq T, \tag{1}$$

where T is the length of a frame, τ_0 is reserved for all SUs to harvest the initial energies and exchange information for network formulation. Obviously, the multiple SUs case can be reduced to a single SU case.

Besides the allocated transmission duration τ_k, SU_k continuously harvests energy in the licensed spectrum. We consider $N \to \infty$ frames to evaluate the long-term average performance of the GCRN. Thus, the energy harvesting duration for SU_k is calculated as $\sum_{i=0, i\neq k}^{M} \tau_i$ and the average harvested energy of SU_k for each time transmission is calculated as

$$E_k = \xi_k P_t h_k \sum_{\substack{i=0 \\ i \neq k}}^{M} \tau_i, \forall k \in \{1, \ldots, M\}, \tag{2}$$

where h_k is the channel power gain on the energy link from PT to SU_k. $0 \leq \xi_k \leq 1$ is the energy conversion efficiency determined by the equipped energy harvester. For convenience, we assume that the energy conversion efficiencies are all equal to ξ, i.e., $\xi_1 = \cdots = \xi_M = \xi$. Note that the noise energy is neglected in Equation (2), since the noise power is negligible compared to P_t.

With the harvested energy, SU_k transmits data to AP in the allocated time τ_k. The received signals at AP can be expressed as

$$y_k = \sqrt{P_k g_k} x_k + \sqrt{P_t h_0} x_p + n_k, \forall k \in \{1, \ldots, M\}, \tag{3}$$

where x_k and x_p are the signals of SU_k and PT, respectively. $n_k \sim \mathcal{CN}(0, N_0)$ is the circularly symmetric complex Gaussian (CSCG) noise with power N_0. g_k is the channel power gain on the information link from SU_k to AP, and h_0 is the channel power gain from PT to AP. P_k is the transmit power of SU_k. Note that P_k must be strictly controlled such that the peak interference power at PR does not exceed the prescribed interference power threshold I_p, i.e.,

$$P_k f_k \leq I_p, \forall k \in \{1, \ldots, M\}, \tag{4}$$

where f_k is the channel power gain on the interference link from SU_k to PR.

Under the interference power constraint of PR, there may be remaining energies after transmission, since SUs may not use up all the harvested energies for transmission. In this article, we ignore the possible remaining energies, since the supercapacitors suffer from serious self-discharge and the transmitter/receiver circuitries of SUs also consume energy. That is to say, there are no initial energy storages at SUs in each communication cycle. Consequently, the obtained performance in this article can be regarded as a floor for the performance of the GCRN with energy storage and management. Future work taking into account energy storage and management will further enhance the performance of GCRNs.

With the allocated τ_k and P_k, the achievable throughput between SU_k and AP is calculated as

$$R_k(\tau_k, P_k) = \tau_k \log_2 \left(1 + \frac{P_k g_k}{P_t h_0 + N_0}\right), \forall k \in \{1, \ldots, M\}, \tag{5}$$

where $\frac{P_k g_k}{P_t h_0 + N_0}$ is the single-to-interference-plus-noise ratio (SINR) at AP imposed by PT and SU_k.

Obviously, for given setup of PUs (i.e., P_t and I_p), the throughput of SU_k is highly dependent upon the channel power gains, which are further influenced by the deployments of SUs. On one hand, h_k, which decides the harvested energy, and f_k, which constrains the transmit power of SU_k, together influence the transmitter of SU_k. On the other hand, h_0, which decides the interference at AP, and g_k, which decides the received information, together influence the receiver of AP. Thus, AP should perform resource allocation according to channel state information (CSI). To this end, we assume that AP can perfectly evaluate the required CSI by channel training and estimation, pilot sensing, direct feedbacks from PUs and SUs, or even indirect feedbacks from a band manager (Rakovic et al. 2015; Xu et al. 2016, 2017). Furthermore, we assume that all SU suffer from quasi-static block fading channels independently, where the channel states keep invariant over each frame.

4 SUM-THROUGHPUT MAXIMIZATION

In this section, we first formulate the sum-throughput maximization (STM) problem in terms of time and power allocation, and then we propose the JOTPA algorithm to obtain the optimal solutions for the STM problem.

By TDMA, the sum-throughput of the GCRN with M SUs is given by

$$\mathcal{R} = \sum_{k=1}^{M} R_k(\tau_k, P_k). \tag{6}$$

Note that the fairness among SUs in the GCRN can be achieved by assigning each SU a weight for transmission, as a result of which a weighted sum-throughput can be obtained. However, as the weights are usually prespecified, we assume the weights of all SUs are equal without loss of generality.

Then, subject to the interference power constraint of PR and the harvested energy constraints of SUs, the STM problem with respect to time and power allocation is formulated as

$$(\text{P1}): \max_{\boldsymbol{\tau},\boldsymbol{\mathcal{P}}} \sum_{k=1}^{M} \tau_k \log_2\left(1+\frac{P_k g_k}{P_t h_0 + N_0}\right), \tag{7}$$

$$\text{s.t. } P_k \tau_k \le \xi P_t h_k \sum_{\substack{i=0 \\ i\neq k}}^{M} \tau_i, \forall k \in \{1,\ldots,M\}, \tag{8}$$

$$0 \le P_k \le \frac{I_p}{f_k}, \forall k \in \{1,\ldots,M\}, \tag{9}$$

$$0 \le \tau_k \le T, \forall k \in \{1,\ldots,M\}, \tag{10}$$

$$\sum_{k=0}^{M} \tau_k \le T, \tag{11}$$

where $\boldsymbol{\tau} = [\tau_0, \tau_1, \tau_2, \ldots, \tau_M]$ and $\boldsymbol{\mathcal{P}} = [P_1, P_2, \ldots, P_M]$ are the vectors of time and power allocation, respectively.

In problem (P1), Equation (8) is the harvested energy constraint imposed by energy harvesting, which means that the allocated energy of SU_k cannot exceed the harvested energy. Equation (9) is the interference power constraint of PR, which indicates that the peak interference power at PR imposed by SU_k cannot exceed the tolerable threshold I_p. Thus, the transmit power of each SU is subject to not only the peak interference power at PR as in common underlay CRNs, but also the harvested energy of SU. Moreover, Equation (10) is the allocated time constraint for each SU, while Equation (11) is the total allocated time constraint as Equation (1).

It should be noticed that, as we study the long-term average performance of the GCRN when $N \to \infty$, the STM problem (P1) is indeed one of N subproblems that stem from an average sum-throughput maximization (ASTM) problem. However, studying the STM problem (P1) can help us gain a comprehensive insight into the average performance (Kang et al. 2011; Hadzi-Velkov et al. 2016). The reasons are explained as follows. In frame j ($j = 1, \ldots, N$), let $\mathcal{R}(j)$ denote the sum-throughput given by Equation (7). Then, the average sum-throughput is calculated as $\bar{\mathcal{R}} = \frac{1}{N}\sum_{j=1}^{N} \mathcal{R}(j)$, which is the objective function of the ASTM problem. Meanwhile, the constraints indexed by j in the ASTM problem are all consistent with those in the STM problem (P1). Obviously, the ASTM problem can be decomposed into N subproblems, each with the same form as the STM problem (P1) with respect to the multiuser resource allocation in a frame. Thus, instead of directly studying the ASTM problem, we study the STM problem (P1) for each frame. For notational convenience, we omit the time index j and consider an arbitrary frame.

To solve problem (P1), we first present the following lemma to show the relationship between the optimal resource allocation and the maximum sum-throughput.

Lemma 4.1. *The sum-throughput of the GCRN with M SUs is maximized only when the total frame time is completely allocated to SUs, namely* $\sum_{k=0}^{M} \tau_k = T$.

Proof. This lemma can be proved by contradiction. We first assume that there is the optimal time allocation $\boldsymbol{\tau}$ satisfying $\sum_{k=0}^{M} \tau_k < T$ and obtaining the maximum sum-throughput $\mathcal{R}(\boldsymbol{\tau}, \boldsymbol{\mathcal{P}})$. Let $\Omega \triangleq T - \sum_{k=1}^{M} \tau_k$ denote the remaining duration in a frame. We divide Ω into two parts as $\Omega = \Omega_1 + \Omega_2$ ($\Omega_1 \ge \Omega_2$), where Ω_1 is added to τ_0 for the energy harvesting of all SUs and Ω_2 is

added to τ_k for the information transmission of SU_k. In this way, both the energy harvesting duration and the information transmission duration of SU_k are enhanced. Furthermore, the transmit power of SU_k can also be enhanced under Equations (8) and (9), as a result of which there must be $P'_k \geq P_k$. It is obvious that $R_k(\tau_k, P_k)$ is a monotonic increasing function of both τ_k and P_k. Let $\tau'_k \triangleq \tau_k + \Omega_2$, there must be $R_k(\tau'_k, P'_k) > R_k(\tau_k, P_k)$. Then, the sum-throughput is enhanced as any increase of $R_k(\tau_k, P_k)$ can enhance $\mathcal{R}(\boldsymbol{\tau}, \boldsymbol{\mathcal{P}})$. This fact is in contrast to the maximum of $\mathcal{R}(\boldsymbol{\tau}, \boldsymbol{\mathcal{P}})$. In this way, we complete the proof of Lemma 4.1. □

Obviously, problem (P1) is non-convex, since there is the product of τ_k and P_k in Equation (8). By introducing an auxiliary optimization variable $e_k = P_k \tau_k$ and substituting constraint Equation (11) with equality by Lemma 4.1 into Equation (8), we can equivalently transform problem (P1) into the following optimization problem:

$$(\text{P2}): \max_{\boldsymbol{\tau}, \boldsymbol{e}} \sum_{k=1}^{M} \tau_k \log_2 \left(1 + \frac{e_k}{\tau_k} \rho_k\right), \tag{12}$$

$$\text{s.t. } e_k \leq \xi P_t h_k (T - \tau_k), \forall k \in \{1, \ldots, M\}, \tag{13}$$

$$0 \leq e_k \leq \frac{\tau_k I_p}{f_k}, \forall k \in \{1, \ldots, M\}, \tag{14}$$

$$0 \leq \tau_k \leq T, \forall k \in \{1, \ldots, M\}, \tag{15}$$

where $\boldsymbol{e} = [e_1, \ldots, e_M]$ is the vector of energy allocation, $\rho_k = \frac{g_k}{P_t h_0 + N_0}$ and $R_k(\tau_k, e_k) = \tau_k \log_2(1 + \frac{e_k}{\tau_k} \rho_k)$ are defined for convenience.

Lemma 4.2. *The sum-throughput $\mathcal{R}(\boldsymbol{\tau}, \boldsymbol{e}) = \sum_{k=1}^{M} R_k(\tau_k, e_k)$ is a jointly concave function of $\boldsymbol{\tau}$ and $\boldsymbol{e}$.*

Proof. For SU_k, the achievable throughput $R_k(\tau_k, e_k)$ is a perspective of $\log_2(1 + e_k \rho_k)$, which is concave over e_k. As the perspective operation preserves convexity (Boyd and Vandenberghe 2004), $R_k(\tau_k, e_k)$ is a jointly concave function of τ_k and e_k. Furthermore, as $\mathcal{R}(\boldsymbol{\tau}, \boldsymbol{e})$ is the pointwise summation of M concave functions, we can conclude that $\mathcal{R}(\boldsymbol{\tau}, \boldsymbol{e}) = \sum_{k=1}^{M} R_k(\tau_k, e_k)$ is a jointly concave function of $(\boldsymbol{\tau}, \boldsymbol{e})$. □

According to Lemma 4.2, the objective function in problem (P2) is a concave function of $(\boldsymbol{\tau}, \boldsymbol{e})$. Moreover, with the help of $\boldsymbol{e}$, the original harvested energy constraint Equation (8) in problem (P1) is also converted into an affine set of $(\boldsymbol{\tau}, \boldsymbol{e})$ as Equation (13) in problem (P2). Thus, the original non-convex problem (P1) in terms of time and power allocation is equivalently transformed into a convex optimization problem (P2) with respect to time and energy allocation. In the following, we solve problem (P2) by convex optimization techniques.

As problem (P2) is a convex optimization problem and satisfies Slater's condition (Boyd and Vandenberghe 2004), the duality gap between the primal problem and the dual problem must be zero. Thus, we solve the dual problem of problem (P2) instead.

The partial Lagrangian function with respect to Equation (13) is formulated as

$$\mathcal{L}(\boldsymbol{\tau}, \boldsymbol{e}, \boldsymbol{\lambda}) = \sum_{k=1}^{M} \tau_k \log_2 \left(1 + \frac{e_k}{\tau_k} \rho_k\right) - \sum_{k=1}^{M} \lambda_k \left(e_k - \xi P_t h_k (T - \tau_k)\right), \tag{16}$$

where $\boldsymbol{\lambda} = [\lambda_1, \ldots, \lambda_M]$ is the nonnegative vector of Lagrange multiplier associated with Equation (13).

Then, the Lagrange dual function of problem (P2) is expressed as

$$\mathcal{G}(\boldsymbol{\lambda}) = \max_{\boldsymbol{\tau}, \boldsymbol{e}} \mathcal{L}(\boldsymbol{\tau}, \boldsymbol{e}, \boldsymbol{\lambda}). \tag{17}$$

Furthermore, the Lagrange dual problem of problem (P2) is given by

$$\min_{\boldsymbol{\lambda} \geq 0} \ \mathcal{G}(\boldsymbol{\lambda}). \tag{18}$$

The optimal solution of problem (P2) is given by the following lemma.

Lemma 4.3. *Let $\boldsymbol{\tau}^* = [\tau_0^*, \tau_1^*, \ldots, \tau_M^*]$ and $\boldsymbol{e}^* = [e_1^*, \ldots, e_M^*]$ denote the vectors of the optimal time and energy allocation, respectively. Given $\boldsymbol{\lambda} \geq 0$, the optimal solution to problem (P2) is given by*

$$e_k^* = \min\left(\left(\frac{\tau_k^*}{\ln 2\lambda_k} - \frac{\tau_k^*}{\rho_k}\right)^+, \frac{I_p \tau_k^*}{f_k}\right), \quad \forall k \in \{1, \ldots, M\}, \tag{19}$$

$$\tau_k^* = \min\left(\left(-\frac{e_k^* \rho_k \mathcal{W}(\psi_k)}{\mathcal{W}(\psi_k) + 1}\right)^+, T\right), \quad \forall k \in \{1, \ldots, M\}, \tag{20}$$

$$\tau_0^* = T - \sum_{k=1}^{M} \tau_k^*, \tag{21}$$

where $(t)^+ \triangleq \max(0, t)$ and $\psi_k = -\exp\left(-(\ln 2\xi P_t \lambda_k h_k + 1)\right)$. $\mathcal{W}(\cdot)$ is the Lambert W function, which is the inverse function of $f(t) = t\exp(t)$ (Corless et al. 1996).

Proof. The Lagrangian function given by Equation (16) can be reformulated as

$$\mathcal{L}(\boldsymbol{\tau}, \boldsymbol{e}, \boldsymbol{\lambda}) = \sum_{k=1}^{M} \mathcal{L}_k(\tau_k, e_k, \lambda_k) + \lambda_k \xi P_t h_k T, \tag{22}$$

where $\mathcal{L}_k(\tau_k, e_k, \lambda_k) = \tau_k \log_2(1 + \frac{e_k}{\tau_k}\rho_k) - \lambda_k e_k - \lambda_k \xi P_t h_k \tau_k$, $\forall k \in \{1, \ldots, M\}$.

To maximize the Lagrangian function in the Lagrange dual function $\mathcal{G}(\boldsymbol{\lambda})$, we should maximize each $\mathcal{L}_k(\tau_k, e_k, \lambda_k)$ subject to Equations (14) and (15), where $\mathcal{L}_k(\tau_k, e_k, \lambda_k)$ only depends on τ_k and e_k for the given λ_k. By the Lagrange dual decomposition, we can solve the following subproblem instead:

$$\text{(P3)}: \ \max_{\tau_k, e_k} \mathcal{L}_k(\tau_k, e_k, \lambda_k), \tag{23}$$

$$\text{s.t. } 0 \leq e_k \leq \frac{\tau_k I_p}{f_k}, \tag{24}$$

$$0 \leq \tau_k \leq T. \tag{25}$$

To solve problem (P3) with the given λ_k, we can calculate e_k for given τ_k and versus τ_k for given e_k. Specifically, given λ_k and τ_k, by calculating the partial derivative of $\mathcal{L}_k(\tau_k, e_k, \lambda_k)$ with respect to e_k and setting $\frac{\partial \mathcal{L}_k(\tau_k, e_k, \lambda_k)}{\partial e_k} = 0$, we can solve e_k as

$$e_k = \left(\frac{1}{\ln 2\lambda_k} - \frac{1}{\rho_k}\right)\tau_k. \tag{26}$$

As the allocated energy e_k is also constrained by Equation (24) in problem (P3), we have the optimal energy allocation as Equation (19).

Similarly, given λ_k and e_k, by deriving $\frac{\partial \mathcal{L}_k(\tau_k, e_k, \lambda_k)}{\partial \tau_k} = 0$, we obtain

$$\ln\left(1 + \frac{e_k}{\tau_k}\rho_k\right) - \frac{\frac{e_k}{\tau_k}\rho_k}{1 + \frac{e_k}{\tau_k}\rho_k} = \ln 2\xi P_t \lambda_k h_k. \tag{27}$$

After some mathematical manipulations, we have

$$-\frac{1}{1+X}\exp\left(-\frac{1}{1+X}\right) = -\exp(-(1+Y)), \tag{28}$$

where $X = \frac{e_k}{\tau_k}\rho_k$ and $Y = \ln 2\xi P_t \lambda_k h_k$ are defined for convenience. Then, with the help of the Lambert W function, we can solve τ_k as

$$\tau_k = -\frac{e_k \rho_k \mathcal{W}(\psi_k)}{\mathcal{W}(\psi_k) + 1}. \tag{29}$$

As the allocated time τ_k is also subject to Equation (25) in problem (P3), we can calculate τ_k as Equation (20). After obtaining τ_k for $k = 1, \ldots, M$, we can calculate τ_0 as $\tau_0 = T - \sum_{k=1}^{M} \tau_k$ according to Lemma 4.1. □

By Lemma 4.3, we propose the joint optimal time and power allocation (JOTPA) algorithm based on iterative Lagrange dual decomposition. The proposed JOTPA algorithm is summarized in Algorithm 1. We first calculate the allocated time and energy for given $\boldsymbol{\lambda}$ and then update $\boldsymbol{\lambda}$ by a sub-gradient algorithm until it converges to a prescribe accuracy. More specifically, given τ_k, $\forall k \in \{1, \ldots, M\}$, we first calculate e_k by Equation (19). Then, with the obtained e_k, we calculate τ_k by Equation (20). In this way, e_k and τ_k are iteratively calculated until they converge to e_k^* and τ_k^* with a prescribed accuracy ε. After obtaining the optimal time allocation for each SU, we can calculate τ_0^* as Equation (21), since $\sum_{k=0}^{K} \tau_k^* = T$, according to Lemma 4.1. Through the above process, we obtain the optimal time and energy allocation $(\boldsymbol{\tau}^*, \boldsymbol{e}^*)$ for the given $\boldsymbol{\lambda}$. Then, we employ the ellipsoid method to find the optimal Lagrange multiplier vector $\boldsymbol{\lambda}^*$ that minimizes $\mathcal{G}(\boldsymbol{\lambda})$. The sub-gradient of $\mathcal{G}(\boldsymbol{\lambda})$ at λ_k is given by

$$\nabla\lambda_k = e_k^* - \xi P_t h_k (T - \tau_k^*), \forall k \in \{1, \ldots, M\}. \tag{30}$$

By solving the Lagrange dual problem of problem (P2), we obtain the maximum sum-throughput with the optimal time and energy allocation $(\boldsymbol{\tau}^*, \boldsymbol{e}^*)$. As problem (P2) is equivalently transformed from problem (P1), the optimal solution of problem (P1) can be calculated from that of problem (P2). With $(\boldsymbol{\tau}^*, \boldsymbol{e}^*)$, we can easily obtain the optimal power allocation $\boldsymbol{\mathcal{P}^*} = [P_1^*, P_2^*, \ldots, P_M^*]$, where $P_k^* = \frac{e_k^*}{\tau_k^*}$, $\forall k \in \{1, \ldots, M\}$.

Algorithm 1 can obtain the optimal solution with guaranteed convergence due to the following reasons. It is obvious that there are two loops in Algorithm 1, wherein the inner loop updates τ_k and e_k for given Lagrange multiplier λ_k and the outer loop updates λ_k by the ellipsoid method. For the inner loop with steps 3–7, τ_k and e_k can converge to the optimum for each given λ_k, since they are iteratively solved for the convex problem (P3). For the outer loop with steps 1–12, according to the convex nature of problem (P2) and the convergence of the ellipsoid method, we can guarantee that the solution converges to the optimum by utilizing the ellipsoid method to update λ_k. As both the inner and outer loops can converge to the optimum, we can conclude that the obtained solution by Algorithm 1 is optimal. As problem (P1) is equivalent to problem (P2), the solution of problem (P1) obtained from that of problem (P2) is also optimal.

Moreover, Algorithm 1 is with finite computational complexity. First, the complexity for updating $(\boldsymbol{\tau}, \boldsymbol{e})$ with the given $\boldsymbol{\lambda}$ is $O(M)$, wherein the complexity for steps 3–7 is $O(M)$ and that for step 9 is $O(1)$. Then, as the ellipsoid method converges in $O(n^2)$ iterations where n is the number of

variables, the complexity for updating $\boldsymbol{\lambda}$ by steps 10–11 is $O(M^2)$. Finally, the complexity to obtain $\mathcal{P}$ by step 13 is $O(1)$. In this way, the total computational complexity of Algorithm 1 is $O(M^3)$.

ALGORITHM 1: Joint Optimal Time and Power Allocation

Input: $\xi, M, T, P_t, I_p, N_0, \varepsilon, g_k, f_k, h_k$;
Output: $(\tau^*, \mathcal{P}^*)$;
1 **repeat**
2 Initialize $\lambda_k \geq 0$, $n \leftarrow 0$, $\tau_k^{(n)}, \forall k \in \{1, \ldots, M\}$;
3 **repeat**
4 Given $\tau_k^{(n)}$, compute e_k by (19), set $e_k^{(n+1)} \leftarrow e_k$;
5 Given $e_k^{(n+1)}$, compute τ_k by (20), set $\tau_k^{(n+1)} \leftarrow \tau_k$;
6 Set $n \leftarrow n + 1$;
7 **until** $||(\tau_k^{(n)}, e_k^{(n)}) - (\tau_k^{(n-1)}, e_k^{(n-1)})||_2 \leq \varepsilon$;
8 Set $(\tau_k^*, e_k^*) \leftarrow (\tau_k^{(n)}, e_k^{(n)})$;
9 Compute τ_0^* by (21) ;
10 Compute the sub-gradient of $\mathcal{G}(\boldsymbol{\lambda})$ at λ_k by (30) ;
11 Update λ_k by the ellipsoid method ;
12 **until** λ_k *converges with a prescribed accuracy*;
13 Compute $P_k^* = \frac{e_k^*}{\tau_k^*}, \forall k \in \{1, \ldots, M\}$;

With the proposed JOTPA algorithm, AP performs optimal resource allocation for SUs and SUs communicate with AP according to the schedule of AP. Specifically, AP first obtains the required CSI and then calculates the optimal resource allocation for given setup of PUs by Algorithm 1. After obtaining the optimal time and power allocation, AP broadcasts the results to SUs. The above process is assumed to be instantaneously accomplished at the beginning of each frame. Finally, each SU transmits data with the allocated transmit power to AP in the allocated time or harvests energy from PT otherwise. In this way, we obtain the maximum sum-throughput by the optimal time and power allocation.

5 SIMULATION RESULTS

In this section, we present simulation results to evaluate the GCRN with JOTPA. Unless otherwise specified, the simulation parameters are set as follows. The length of a frame is normalized as $T = 1$. The number of SUs is set as $M = 3$. The energy conversion efficiency is set as $\xi = 0.8$. The noise power is set as $N_0 = 1$, while both P_t and I_p are normalized by N_0. The transmit power of PT is set as $P_t = 40$dB, while the peak interference power at PR is set as $I_p = 5$dB. For the channel model, both large scale path loss and small scale channel fading are taken into consideration. The channel power gain can be expressed as $u = \beta_u(\frac{d_u}{d_0})^{-\alpha} (u = h_k, g_k, f_k)$, where β_u and d_u are the channel fading gain and the distance for energy link h_k, information link g_k and interference link f_k, d_0 is the reference distance, α is the path loss exponent. We set $d_0 = 1$ and $\alpha = 2$ without loss of generality. The channel fading is modeled as independent Rayleigh block fading, as a result of which β_u is an exponential random variable. During the simulation, we mainly consider three GCRN deployments as depicted in Figure 3, according to which d_u can be calculated. By evaluating the GCRN in these three typical deployments, we can gain a comprehensive insight into its performance.

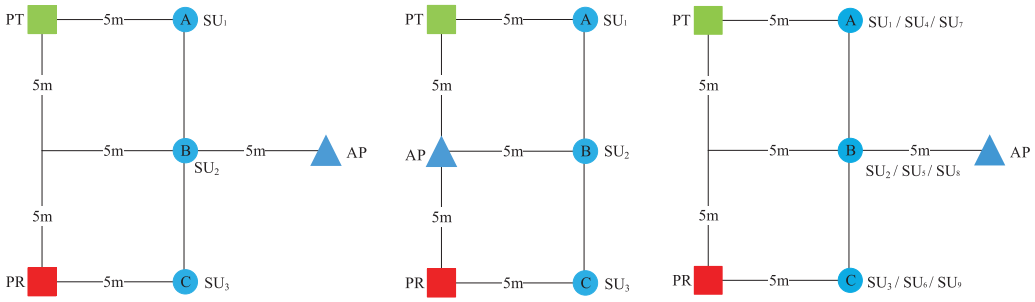

Fig. 3. Different deployments of the GCRN.

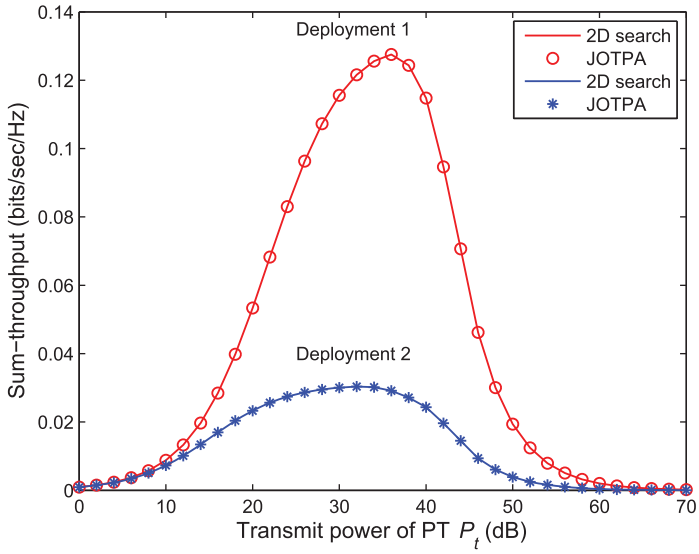

Fig. 4. Sum-throughput versus the transmit power of PT in different deployments.

In Figure 4, we first collaborate the effectiveness of the proposed JOTPA algorithm by comparing it with a two-dimensional exhaustive search algorithm that obtains the optimum with high computational complexity. It is obvious that there is an excellent agreement between the two algorithms, which validates the optimality of JOTPA. Then, we study the impact of PT on the sum-throughput of the GCRN. When P_t is small (e.g., $P_t < 10$dB), the sum-throughput is also small as the harvested energies by SUs are limited. With the increase of P_t, more energies are harvested by SUs and a larger sum-throughput is achieved. However, when P_t becomes very large (e.g., $P_t > 38$dB), the sum-throughput begins to decrease as the interference of PT at AP keeps on increasing while the transmit powers of SUs cannot be further enhanced due to the constraint of I_p. For this case, the harvested energies by SUs cannot be totally used for transmission but are discharged due to the leakage of supercapacitors. Thus, we can conclude that too large P_t cannot benefit SUs more but interfere with AP more. Overall, the sum-throughput first increases and then decreases with the increase of P_t. Finally, we compare the sum-throughput of the GCRNs in Deployment 1 and Deployment 2 as depicted in Figures 3(a) and 3(b), respectively. Note that the AP in Deployment 2 is nearer to PT than that in Deployment 1. Thus, the AP in Deployment

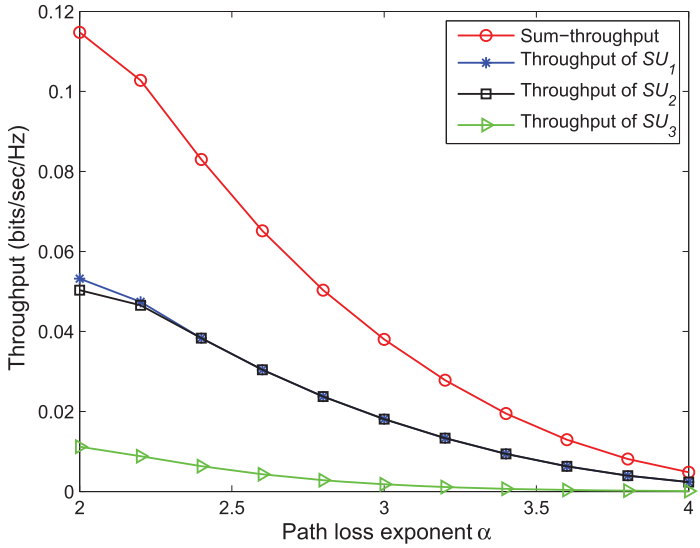

Fig. 5. Throughput versus path loss exponent in Deployment 1.

2 suffers more interference from PT and the sum-throughput of Deployment 2 is always smaller than that of Deployment 1 no matter P_t is large or small. As such, if AP is deployed properly, SUs will not suffer from the "doubly near-far" problem in WPCNs (Ju and Zhang 2014b) wherein the energy transmitter and the information receiver are co-located in a hybrid AP.

Figure 5 investigates the impact of path loss on the throughput of the GCRN in Deployment 1. Obviously, the throughput of each SU and the sum-throughput of the GCRN all decrease with the increase of path loss exponent, since the path loss significantly influences the harvested energies of SUs and the received information of AP. If the path loss becomes severe, then less energies can be harvested by SUs and less information can be correctly received by AP, which certainly decreases the throughput of each SU and the sum-throughput of the GCRN. Moreover, we can observe that both SU_1 and SU_2 obtain larger throughput than SU_3, since they suffer from different path losses. More specifically, SU_1, which is nearer to PT but farther from PR, suffers from smaller path loss on the energy link and larger path loss on the interference link than SU_3 on the contrary. Consequently, SU_1 gains more energy from PT and less constraint from PR than SU_3. However, SU_1 and SU_3 suffer larger path losses on the information links to AP than SU_2, where the position of SU_2 is a compromise of SU_1 and SU_3. Thus, SU_2 obtains a similar throughput as SU_1 by JOTPA, while SU_3 obtains much less throughput than SU_1 and SU_2.

In Figure 6, we compare the GCRN with different energy conversion efficiencies under different interference power constraints of PR. As shown, the sum-throughput is very small when the interference power constraint of PR is strict (i.e., I_p is small). The reason is that even though the harvested energies by SUs may be sufficient, the transmit powers of SUs cannot be set too large such that PR can be protected sufficiently. Then, with the slack of the interference power constraint, namely I_p increases, the sum-throughput increases as more harvested energies can be utilized for transmission. However, when I_p is large enough (e.g., $I_p > 10$dB), the sum-throughput saturates without further increasing. This is because, for the given P_t, all the harvested energies of SUs are allocated to maximize their transmit powers in the allocated time and no more energies are available to further enhance the transmit powers of SUs. For this case, the GCRN is equivalent to a WPCN without interference power constraint. In addition, it is also obvious that a larger ξ results in a larger sum-throughput, since more energies can be harvested and allocated by SUs.

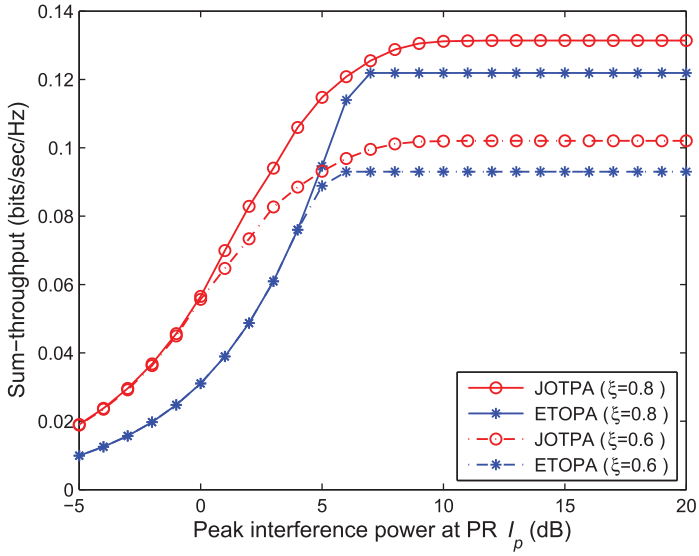

Fig. 6. Sum-throughput versus the peak interference power at PR for JOTPA and ETOPA with different energy conversion efficiencies in Deployment 1.

Figure 6 further validates the superiority of JOTPA by comparing it with the equal time and optimal power allocation (ETOPA) algorithm, which follows typical TDMA networks that allocate time equally and common underlay CRNs that allocate power with the consideration of the peak interference power at PR and the maximum transmit powers of SUs. It is obvious that JOTPA outperforms ETOPA no matter what I_p or ξ is set. This is due to the fact that ETOPA does not allocate time according to the setup of PUs and CSI, which results in the unbalanced energy distribution among SUs. In this way, the harvested energies for some SUs are not enough to reach the peak interference power at PR while for other SUs are too many to be used up for transmission. The above fact further brings about the phenomenon that the sum-throughput of ETOPA saturates more quickly than that of JOTPA.

More specifically, Figure 7 compares the energy statuses of SUs with different resource allocation algorithms under different interference power constraints. Obviously, from SU_1 to SU_3, both the harvested and the allocated energies are decreasing, since the path losses on the energy links are decreasing while those on the interference links are increasing. Comparing Figure 7(a) with Figure 7(b), we can observe that, at each SU, the harvested energies by ETOPA under different interference power constraints are the same while those by JOTPA are not. This is because ETOPA allocates time equally while JOTPA allocates time according to the setup of PUs and CSI. In Figure 7(a), SUs only allocate parts of the harvested energies for transmission, since the transmit powers of SUs are strictly controlled such that the peak interference power at PR is no larger than I_p = 5dB. By contrast, in Figure 7(b), when the interference power constraint is relaxed to I_p = 10dB, all the harvested energies are allocated, since SUs can utilize more energies for transmission. For any case, even though the harvested energies of some SUs by ETOPA may be larger than those by JOTPA, the total allocated energy of all SUs by ETOPA is much smaller than that by JOTPA, which indicates that JOTPA outperforms ETOPA in green energy utilization.

To further evaluate the performance of the GCRN with multiple SUs, we depict Figure 8 to present the relationship between the sum-throughput and the number of SUs. The deployments of SUs follow Figure 3(c), in which SU_1–SU_9 are sequentially placed at positions A, B, and C. We

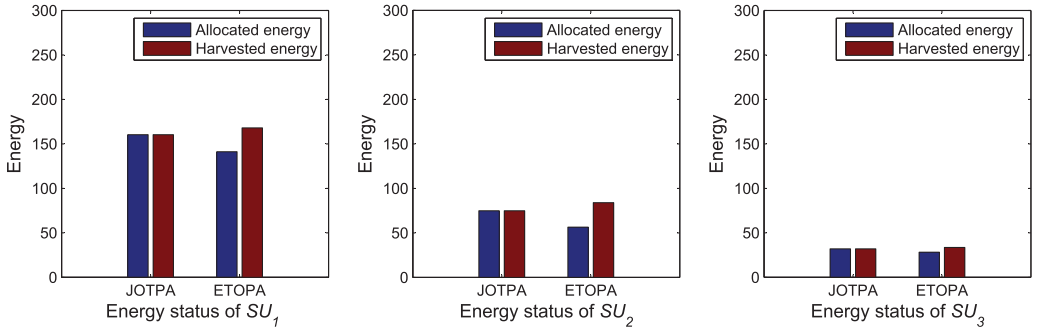

(a) Energy statuses the GCRN with JOTPA and ETOPA: $I_p = 5$ dB

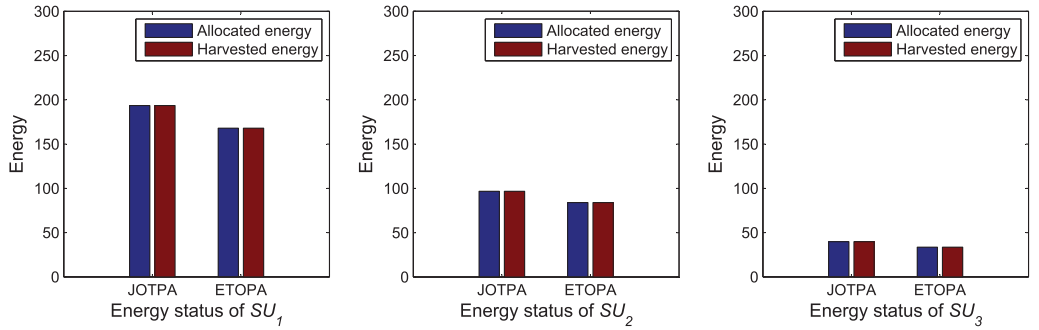

(b) Energy statuses of the GCRN with JOTPA and ETOPA: $I_p = 10$ dB

Fig. 7. Energy statuses of the GCRN with different interference power constraints in Deployment 1.

can observe that the sum-throughput is not always increasing with the increase of M. For both JOTPA and ETOPA, the sum-throughput gains of adding SUs at position A or B are much larger than those of adding SUs at position C. The reasons can be explained as follows. SUs at position C suffer larger path losses on the energy links and the information links but smaller path losses on the interference links, as a result of which SUs at position C contribute less throughput to the sum-throughput than other SUs at position A or B. For ETOPA, when $M > 2$, adding SUs at position C will even decrease the sum-throughput, since the frame is equally divided and SUs with the same duration at different positions make different contributions to the sum-throughput. Specifically, when a SU is added at position C, the frame must be allocated again, as a result of which the transmission durations of other SUs are decreased. However, the throughput gain of adding SU at position C cannot compensate the throughput losses of other SUs, which certainly decreases the sum-throughput. In contrast, for JOTPA, the sum-throughput never decreases even adding SUs at position C. This is because JOTPA may not allocate time to SUs at position C according to the setup of PUs and CSI. As a result, JOTPA is always superior to ETOPA, which verifies the superiority of the proposed JOTPA algorithm.

6 CONCLUSION

In this article, we investigated an underlay GCRN, wherein multiple battery-free SUs harvest energy from the RF signals of PUs and sequentially transmit data to AP concurrently with PUs, all in the licensed spectrum. In this way, SUs could utilize both the spectrum and the energy of PUs to enhance spectrum efficiency and green energy utilization. Under this setup, we formulated the

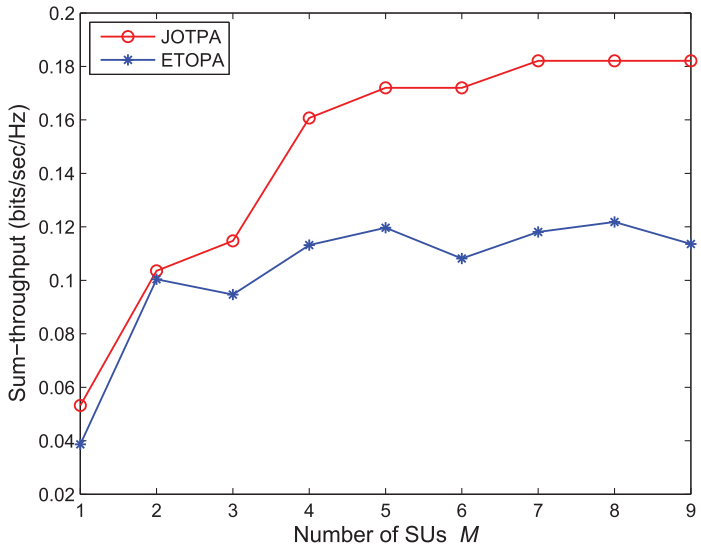

Fig. 8. Sum-throughput versus the number of SUs for JOTPA and ETOPA in Deployment 3.

sum-throughput maximization problem subject to the interference power constraint of PR and the harvested energy constraints of SUs. To solve this non-convex problem, we proposed the JOTPA algorithm based on the iterative Lagrange dual decomposition and obtained the optimal time and power allocation. By studying how the setup of PUs and the deployment of SUs impact the GCRN, we observed that SUs close to PT and AP but far from PR can contribute more throughput to the sum-throughput than other SUs, and SUs cannot always benefit from PUs. These observations could guide us to deploy the GCRN properly. Moreover, by making comparisons between JOTPA and ETOPA, we collaborated that JOTPA outperforms ETOPA in green energy utilization and can satisfy large number of SUs without sum-throughput decreasing.

REFERENCES

Suzhi Bi, Chin Keong Ho, and Rui Zhang. 2015. Wireless powered communication: Opportunities and challenges. *IEEE Commun. Mag.* 53, 4 (2015), 117–125.

Stephen Boyd and Lieven Vandenberghe. 2004. *Convex Optimization*. Cambridge University Press.

Yongbo Cheng, Pengcheng Fu, Yuchao Chang, Baoqing Li, and Xiaobing Yuan. 2016. Joint power and time allocation in full-duplex wireless powered communication networks. *Mobile Info. Syst.* (2016), 1–15.

Wonsuk Chung, Sungsoo Park, Sungmook Lim, and Daesik Hong. 2014. Spectrum sensing optimization for energy-harvesting cognitive radio systems. *IEEE Trans. Wireless Commun.* 13, 5 (2014), 2601–2613.

R. M. Corless, G. H. Gonnet, D. E. G. Hare, D. J. Jeffrey, and D. E. Knuth. 1996. On the Lambert W function. *Adv. Comput. Math.* 5, 1 (1996), 329–359.

Andrea Goldsmith, Syed Ali Jafar, Ivana Marić, and Sudhir Srinivasa. 2009. Breaking spectrum gridlock with cognitive radios: An information theoretic perspective. *Proc. IEEE* 97, 5 (2009), 894–914.

Yu Gu, Liang He, Ting Zhu, and Tian He. 2014. Achieving energy-synchronized communication in energy-harvesting wireless sensor networks. *ACM Trans. Embed. Comput. Syst.* 13, 2s (2014), 68:1–68:26.

Zoran Hadzi-Velkov, Ivana Nikoloska, George K. Karagiannidis, and Trung Q. Duong. 2016. Wireless networks with energy harvesting and power transfer: joint power and time allocation. *IEEE Signal Process. Lett.* 23, 1 (2016), 50–54.

Peter He and Lian Zhao. 2015. Optimal power control for energy harvesting cognitive radio networks. In *Proceedings of IEEE International Conference on Communications (ICC'15)*. IEEE, 92–97.

Jianwei Huang, Randall A. Berry, and Michael L. Honig. 2006. Auction-based spectrum sharing. *Mobile Netw. Appl.* 11, 3 (2006), 405–418.

Xueqing Huang, Tao Han, and Nirwan Ansari. 2015. On green-energy-powered cognitive radio networks. *IEEE Commun. Surveys Tutor.* 17, 2 (2015), 827–842.

Sobia Jangsher, Haojie Zhou, Victor O. K. Li, and Ka-Cheong Leung. 2015. Joint allocation of resource blocks, power, and energy-harvesting relays in cellular networks. *IEEE J. Sel. Area Commun.* 33, 3 (2015), 482–495.

Hyungsik Ju and Rui Zhang. 2014a. Optimal resource allocation in full-duplex wireless-powered communication network. *IEEE Trans. Commun.* 62, 10 (2014), 3528–3540.

Hyungsik Ju and Rui Zhang. 2014b. Throughput maximization in wireless powered communication networks. *IEEE Trans. Wireless Commun.* 13, 1 (2014), 418–428.

Xin Kang, Chin Keong Ho, and Sumei Sun. 2015. Full-duplex wireless-powered communication network with energy causality. *IEEE Trans. Wireless Commun.* 14, 10 (2015), 5539–5551.

Xin Kang, Rui Zhang, Ying-Chang Liang, and Hari Krishna Garg. 2011. Optimal power allocation strategies for fading cognitive radio channels with primary user outage constraint. *IEEE J. Sel. Area Commun.* 29, 2 (2011), 374–383.

Seunghyun Lee and Rui Zhang. 2015. Cognitive wireless powered network: Spectrum sharing models and throughput maximization. *IEEE Trans. Cogn. Commun. Netw.* 1, 3 (2015), 335–346.

Seunghyun Lee, Rui Zhang, and Kaibin Huang. 2013. Opportunistic wireless energy harvesting in cognitive radio networks. *IEEE Trans. Wireless Commun.* 12, 9 (2013), 4788–4799.

Ying-Chang Liang, Yonghong Zeng, Edward C. Y. Peh, and Anh Tuan Hoang. 2008. Sensing-throughput tradeoff for cognitive radio networks. *IEEE Trans. Wireless Commun.* 7, 4 (2008), 1326–1337.

Ren-Shiou Liu, Prasun Sinha, and Can Emre Koksal. 2010. Joint energy management and resource allocation in rechargeable sensor networks. In *Proceedings of IEEE International Conference on Computer Communications (INFOCOM'10)*. IEEE, 1–9.

Sudha Lohani, Roya Arab Loodaricheh, Ekram Hossain, and Vijay K. Bhargava. 2016. On multiuser resource allocation in relay-based wireless-powered uplink cellular networks. *IEEE Trans. Wireless Commun.* 15, 3 (2016), 1851–1865.

Valentin Rakovic, Daniel Denkovski, Zoran Hadzi-Velkov, and Liljana Gavrilovska. 2015. Optimal time sharing in underlay cognitive radio systems with RF energy harvesting. In *Proceedings of IEEE International Conference on Communications (ICC'15)*. IEEE, 7689–7694.

Sujesha Sudevalayam and Purushottam Kulkarni. 2011. Energy harvesting sensor nodes: Survey and implications. *IEEE Commun. Surveys Tutor.* 13, 3 (2011), 443–461.

Muhammad Usman and Insoo Koo. 2014. Access strategy for hybrid underlay-overlay cognitive radios with energy harvesting. *IEEE Sensors J.* 14, 9 (2014), 3164–3173.

X. Wang, K. Ma, Q. Han, Z. Liu, and X. Guan. 2012. Pricing-based spectrum leasing in cognitive radio networks. *IET Networks* 1, 3 (2012), 116–125.

Ying Wang, Wenxuan Lin, Ruijin Sun, and Yongjia Huo. 2015. Optimization of relay selection and ergodic capacity in cognitive radio sensor networks with wireless energy harvesting. *Pervas. Mobile Comput.* 22 (2015), 33–45.

Yuan Wu and Danny H. K. Tsang. 2009. Distributed power allocation algorithm for spectrum sharing cognitive radio networks with QoS guarantee. In *Proceedings of IEEE International Conference on Computer Communications (INFOCOM'09)*. IEEE, 981–989.

Chi Xu, Meng Zheng, Wei Liang, Haibin Yu, and Yiang-Chang Liang. 2016. Outage performance of underlay multihop cognitive relay networks with energy harvesting. *IEEE Commun. Lett.* 20, 3 (2016), 1148–1151.

Chi Xu, Meng Zheng, Wei Liang, Haibin Yu, and Yiang-Chang Liang. 2017. End-to-end throughput maximization for underlay multi-hop cognitive radio networks with RF energy harvesting. *IEEE Trans. Wireless Commun.* 16, 6 (2017), 3561–3572.

Sixing Yin, Zhaowei Qu, and Shufang Li. 2015. Achievable throughput optimization in energy harvesting cognitive radio systems. *IEEE J. Sel. Area Commun.* 33, 3 (2015), 407–422.

Sixing Yin, Zhaowei Qu, Zhi Wang, and Lihua Li. 2017. Energy-efficient cooperation in cognitive wireless powered networks. *IEEE Commun. Lett.* 21, 1 (2017), 128–131.

Tian Zhang and Wei Chen. 2016. Delay-optimal data transmission in renewable energy aided cognitive radio networks. In *Proceedings of IEEE Wireless Communications and Networking Conference (WCNC'16)*. IEEE, 1–6.

Meng Zheng, Chi Xu, Wei Liang, and Haibin Yu. 2016. Harvesting-throughput tradeoff for RF-powered underlay cognitive radio networks. *Electron. Lett.* 52, 10 (2016), 881–883.

Received June 2016; revised March 2017; accepted May 2017